CHEMISTRY OF MATERIALS
Article
Cite This: Chem. Mater. XXXX, XXX, XXX-XXX
pubs.acs.org/cm

Suppressing the Thermal and Ultraviolet Sensitivity of Kevlar by Infiltration and Hybridization with ZnO

Itxasne Azpitarte,[†] Ana Zuzuarregui,[†] Hayrensa Ablat,[‡] Leire Ruiz-Rubio,[§] Alberto López-Ortega,[†] Simon D. Elliott,[‡] and Mato Knez*[,†,∥]

[†]CIC nanoGUNE, Tolosa Hiribidea, 76, 20018 Donostia-San Sebastián, Gipuzkoa, Spain

[‡]Tyndall National Institute, University College Cork, Lee Maltings, Dyke Parade, Cork, Ireland

[§]Laboratorio de Quimica Macromolecular (Labquimac), Dpto. Quimica-Fisica, Facultad de Ciencia y Tecnologia, Universidad del Pais Vasco, 48940 Leioa, Vizcaya, Spain

[∥]IKERBASQUE, Basque Foundation for Science, 48011 Bilbao, Biscay, Spain

Supporting Information

ABSTRACT: Polyaramides, such as Kevlar, are of great technological importance for their extraordinary mechanical performance. As fibers, they are used in personal safety, for reinforcement of tires and ropes, and in further material composites that require extreme mechanical stability. However, the properties of the polymer depend on the environmental conditions. Specifically, elevated temperatures and/or irradiation with UV light seriously affect its toughness. Classical approaches to protect polyaramide fibers from these external factors rely on coatings with resins or metal oxides, which typically increase the weight and reduce the flexibility of the polymer. Here, we present a bioinspired approach to stabilize the mechanical properties of the polyaramide. With our solvent free vapor phase approach, zinc oxide is infiltrated into the polymer structure, resulting in intermolecular cross-linking of the polymer chains. The procedure results in an increased degradation temperature of the polyaramide, while at the same time it protects the fibers against UV-induced degradation. The chemical interaction between the zinc oxide and the polymer is theoretically modeled, and a chemical structure of the resulting organic−inorganic hybrid material is proposed.

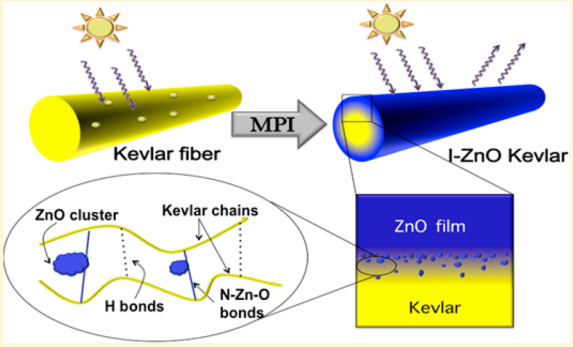

1. INTRODUCTION

Nature is a source of inspiration for the fabrication of a plethora of functional materials. Among the most important functionalities in natural materials are the mechanical properties, which in the course of billions of years of evolution have been optimized in various ways in order to fulfill the needs of a species in a specific environment. The optimization may involve structural features, such as the honeycomb structures,[1,2] structural and compositional features, such as bones or shells,[3,4] or dominantly compositional features. The last of these usually involves the incorporation of metals, such as Zn, Cu, and Mn, into protein matrices, which result in exceptional improvement of the strength or hardness of the protein.[5−7] The aforementioned metals play a crucial role in the enhanced hardness of the jaw, mandibles, and claws of many insects. It is reasonable to assume that intentional incorporation of metals into artificial soft matter may also have positive effects on its mechanical properties. To achieve that, numerous strategies have been established, including wet chemical approaches or technical processing with vaporized chemicals. Especially vapor phase processing has been shown to greatly improve the toughness of some biopolymers (such as spider silk,[8] collagen,[9] and cellulose[10]) through inclusion of very simple metal organic molecules into the proteins or polysaccharides. However, the impact of this strategy on high-strength synthetic polymers of technological importance has never been reported.

Polymeric fibers with high strength are often called upon whenever a material with extraordinary mechanical performance is needed. Among such polymers, poly(*p*-paraphenylene terephthalamide) (Kevlar) is most prominent for its great mechanical toughness without the need of complex processing. The origin of the extraordinary properties lies in Kevlar's unique chemical structure (Figure 1); the rigidity and repetitiveness of its molecular backbone, together with the *para* substitution of the benzene rings, allow the formation of intermolecular hydrogen bonds resulting in an almost perfect monoclinic crystalline packaging. Due to this inherent feature, Kevlar shows liquid crystal-like behavior, such as great tensile strength, strong energy absorption, and thermal insulation. Such outstanding properties in a material with great flexibility and low weight have made Kevlar the material of choice in

Received: September 4, 2017
Revised: November 7, 2017
Published: November 7, 2017

DOI: 10.1021/acs.chemmater.7b03747
Chem. Mater. XXXX, XXX, XXX−XXX

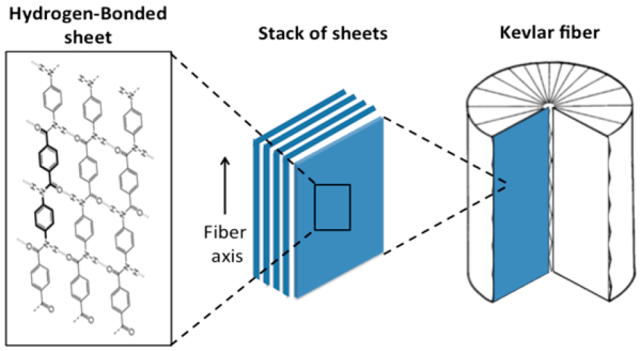

Figure 1. Schematic of the hierarchical structure of Kevlar showing the highly ordered packing of the polymer chains.

many application fields including personal protection, sports equipment, and aerospace.

In many of these applications, Kevlar is exposed to harsh environmental conditions, including high temperature, UV radiation, and/or moisture which often degrade its mechanical properties.[11−15] In order to prevent the loss of mechanical properties, various approaches have been evaluated, most of them based on coating Kevlar fibers with a resin or a metal oxide.[16−20] The drawback of such coatings is on the one hand the extra weight of the resin and on the other hand the reduced flexibility upon coatings with brittle metal oxides. Therefore, development of new routes for protection of Kevlar from thermal and UV-induced degradation along with preservation of its weight and flexibility are in high demand.

Atomic layer deposition (ALD)[21] has been used before to deposit UV absorbing coatings on fabrics and fibers. This technique offers the possibility to create conformal coatings at lower temperatures than other vapor phase deposition techniques with a great control over the thickness of the deposit. However, the materials used for UV protection by ALD are dominantly brittle ceramics and therefore could crack and detach from the fibers upon further mechanical processing or handling. In this work, we present a new approach for the stabilization of the mechanical properties of Kevlar fibers based on vapor phase infiltration of the fiber with a metal oxide. More precisely, we use a modification of ALD known as multiple pulsed infiltration (MPI)[8,22] to infiltrate zinc oxide into Kevlar in analogy with many naturally occurring hybrid biomaterials. With this innovative route, an organic−inorganic hybrid material is created in the subsurface area of Kevlar, thus protecting the fibers from thermal and UV-induced degradation without compromising the desired lightness and flexibility. We compare the properties of ZnO infiltrated fibers with those of ZnO coated fibers to demonstrate the advantages of this new approach.

2. EXPERIMENTAL SECTION

2.1. Sample Preparation. The examined Kevlar fibers were obtained from the woven material commercially used in bulletproof vests (Kevlar 29). The fibers had diameters of 10 μm and were cut to lengths of 3 cm for the experiments.

The modification of the samples was performed in a commercial ALD reactor (Savannah S100, Cambridge NanoTech Inc.). Both infiltration and coating of the fibers were carried out at 150 °C under a constant nitrogen gas flow of 20 standard cubic centimeters per minute (sccm). Diethyl zinc (DEZ, $Zn(Et)_2$, Strem Chemicals) was used as the zinc source and demineralized water as the oxygen source. The coated fibers were prepared following a typical ALD process with a cycle consisting of pulse (DEZ, 0.08 s)/purge (N_2, 30 s)/pulse (H_2O, 0.08 s)/purge (N_2, 30 s). By contrast, the infiltrated fibers were prepared by MPI. In the MPI case the substrate was exposed to the precursors for defined periods of time before purging, thereby allowing diffusion of the precursors into the polymer. An MPI cycle consisted of pulse (DEZ, 0.08 s)/ exposure (30 s)/purge (N_2, 30 s)/pulse(H_2O, 0.08 s)/exposure (30 s)/purge(N_2, 30 s). In both cases, the number of repetitive ALD/MPI cycles was 200.

2.2. TEM/EDS. TEM characterization and EDS analysis were carried out with an FEI Titan microscope using 300 kV in STEM mode and an EDAX SDD detector.

FIB lamellae were prepared by gently stretching the kevlar fibers across a convex aluminum SEM stub (prepared in-house) and fixing it in place at each end using carbon tape. Once the location for the block extraction had been chosen the fiber was further fixed to the substrate with Pt depositions and the block was extracted by standard methods. A Pt electron beam deposition was used initially to protect the sample surface before any ion beam deposition was carried out. The block was thinned to transparency on a copper "Omniprobe" grid using a 5 kV gallium ion beam at 8 pA for final surface preparation.

2.3. DFT Calculations. Density functional theory (DFT) was used to compute the electronic structure of oligomers of Kevlar and ZnO-infiltrated Kevlar in vacuum. The Perdew−Burke−Ernzerhof (PBE) exchange-correlation functional[23] was used with the SV(P) basis set (split valence with polarization at all non-hydrogen atoms) as implemented in TURBOMOLE[24] with the resolution of the identity (RI) approximation for Coulomb integrals[25] accompanied by the corresponding auxiliary basis sets.[26] The "m4" integration grid of the module RIDFT was used.[27,28] Geometries were freely optimized using redundant internal coordinates[29] until gradients were $<10^{-6}$ Hartree/Bohr. Optimized structures were visualized with Materials Studio version 7.0.

The computed system was composed of a total of eight rings of Kevlar in the gas phase. Two adjacent oligomers, each consisting of four covalently bound monomers, were connected via three hydrogen bonds. This meant that the two central monomers of each oligomer, along with the central hydrogen bond, are likely to experience an environment representative of the polymer chain. Computing the structure in the gas phase meant that the geometry of the oligomers with and without ZnO could be freely optimized without imposing any particular periodic lattice. To model the infiltrated sample, the H of all three hydrogen bonds were replaced with [Zn(OH)] cross-links.

2.4. X-ray Diffraction (XRD). The XRD patterns of the samples were measured with a PANalytical X'Pert Pro diffractometer with Cu Kα radiation. For an easier measurement, Knitted fabric Kevlar pieces were analyzed, instead of individual fibers.

2.5. Attenuated Total Reflectance−Fourier Transform Infrared Spectroscopy (ATR-FTIR). The FTIR spectra were carried out in a PerkinElmer Frontier spectrometer with the ATR sampling stage. All spectra were measured with 20 scans from 520 to 4000 cm^{-1} at 4 cm^{-1} resolution. Each sample was measured five times, and the results were averaged.

The spectra were processed using Origin 7.0 to calculate the fwhm of some peaks.

2.6. Thermogravimetric Analysis (TGA). The thermal stabilities of the samples were analyzed using a DTG-60 Shimadzu Thermobalance. The samples (5−10 mg) were heated from room temperature to 700 °C. The scanning rate was 10 °C·min^{-1}, and all measurements were carried out under nitrogen atmosphere.

2.7. Tensile Tests. The tensile tests were done with a BRUKER Universal Mechanical Tester with a resolution of 50 μN and in accordance to the ASTM standard C1557-03 (2008). The fibers were fixed in a cardboard sampler holder, which had a punched hole of 6 mm diameter in the center (Figure S1). After vertical alignment of the fiber across the hole, the sample holder was positioned in the mechanical tester with the fiber being unstrained. Finally, the sample holder was cut along the central guides and tensile force was applied until rupture of the fiber, while the strain was measured simultaneously.

DOI: 10.1021/acs.chemmater.7b03747
Chem. Mater. XXXX, XXX, XXX−XXX

To determine the stability of the fibers under UV light the samples were exposed to light with a wavelength of 365 nm for 24 h. Subsequently the strain−stress curves were measured and compared with the mechanical properties of unexposed fibers.

3. RESULTS AND DISCUSSION

We applied tensile tests to native, thermally treated (ref. Kevlar), ZnO-coated (C-ZnO), and ZnO-infiltrated (I-ZnO) Kevlar fibers. Their resulting moduli of toughness are shown in Figure 2. Thermal treatment refers to constant heating of native

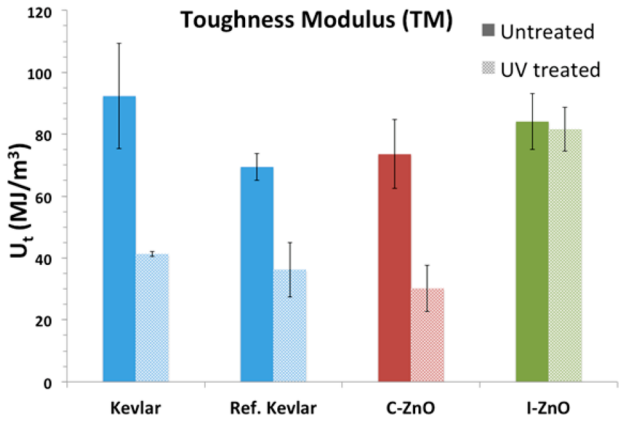

Figure 2. Modulus of toughness of the various processed samples before and after UV irradiation.

Kevlar fibers at 150 °C for 7 h, which should simulate the conditions the fibers experience during the coating or infiltration processes and at the same time should demonstrate the thermal sensitivity of this material. Native Kevlar fibers showed high thermal sensibility retaining only 75% of the initial modulus of toughness after thermal treatment. The ZnO coating was insufficient for the thermal protection of Kevlar as the ZnO-coated fibers retained only 79% of the modulus. The infiltrated sample, however, maintained exceptional values of 91% of the modulus of toughness.

After assessing the benefit of the infiltration on the thermal sensitivity, we additionally exposed the fibers to UV radiation for 24 h before performing the tensile tests. The comparison of the modulus of toughness before and after exposure to UV light shows the high sensitivity of Kevlar to such irradiation. The modulus of toughness of both untreated and heated Kevlar decreased by nearly 50%. In the case of C-ZnO fibers, an even stronger loss of the modulus of around 65% was observed. In contrast, the infiltration with ZnO effectively suppressed UV induced degradation; the I-ZnO fibers retained 90% of the initial modulus of toughness.

The processing conditions are of critical importance for the performance of the resulting polymer. In our case, we used the residence time of the organometallic precursors in the reactor as a variable, being the only process parameter that distinguishes C-ZnO from I-ZnO. A prolonged residence time of DEZ increases the exposure time and as a consequence allows diffusion of the precursor into the interior of the polymer rather than only binding to its surface. In order to illustrate the effect we cross-sectioned the C-ZnO and I-ZnO fibers with a focused ion beam and investigated the cross sections by TEM. The TEM-EDS images (insets in Figure 3) show a clear difference between the coated and the infiltrated sample, specifically at the interface between the ZnO layer and

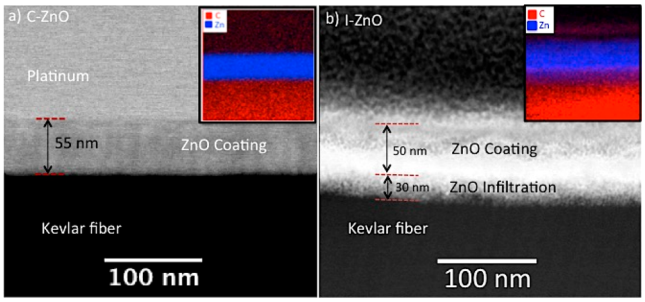

Figure 3. TEM images of cross sections of (a) C-ZnO and (b) I-ZnO fibers. Insets show EDS color maps with the carbon signal coded red and the zinc signal coded blue.

the fiber surface. In the case of C-ZnO, this interface is sharp and clear, while in case of I-ZnO, it is blurred with a gradual decay of the Zn signal down to 30 nm depth below the Kevlar surface. In this subsurface area, the Zn seems to be distributed as a ZnO network embedded into the polymer. It is interesting that this tiny layer of intermixed organic−inorganic material, only about 30 nm thick, significantly enhances the stability and performance of Kevlar.

To understand how the ZnO infiltration positively influences the thermal stability of Kevlar it is necessary to first understand how the elevated temperature affects the native polymer. In spite of several differing interpretations on the mechanism,[30−33] most authors agree that high temperatures disrupt the intermolecular hydrogen bonds leading to a weakening of Kevlar. The H bonding is apparently key for the thermal sensitivity of Kevlar. Based on the observation that the fibers are stabilized for elevated temperatures, it is safe to assume that the ZnO infiltration may result in replacement of the H bonds, likely by covalent N−Zn−O bonds.

The possibility of such chemical reactions between the ALD precursors and the polymer backbone was modeled by density functional theory (DFT). The reaction pathway is schematically shown in Figure 4a. Previous studies of ZnO ALD[34,35] indicate that DEZ adsorbs to Lewis basic sites (such as carbonyl O or amide N of Kevlar) and that transfer of the most acidic proton (here the amide NH) causes an ethyl ligand to be eliminated as ethane. The remaining ligand is eliminated in the H_2O pulse,

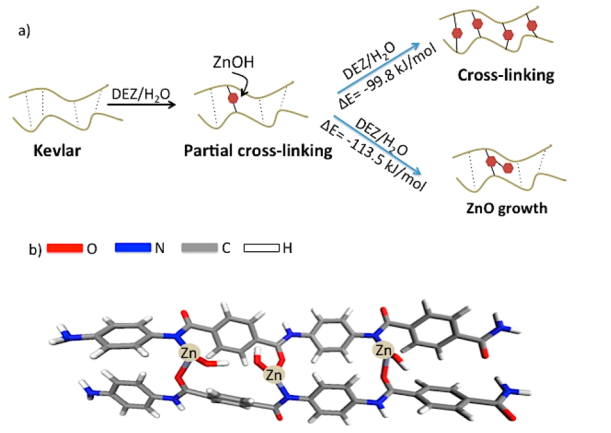

Figure 4. (a) Schematic of the proposed reaction pathways of Kevlar with DEZ and H_2O resulting from the energetically most favored DFT-calculated chemical interactions. (b) Structure of the cross-linked I-ZnO Kevlar oligomer computed with DFT.

DOI: 10.1021/acs.chemmater.7b03747
Chem. Mater. XXXX, XXX, XXX−XXX

producing an OH group on Zn. The net effect is therefore to replace the amide H^+ of Kevlar with $[Zn(OH)]^+$. In standard ALD, this hydroxyl group would react during next DEZ pulse, acting as a nucleus for the growth of a cluster or film of ZnO.

In a model system of two adjacent Kevlar strands, the amide protons were replaced with $[Zn(OH)]^+$ so as to simulate the first MPI pulse, and the lowest energy optimized structure is shown in Figure 4b. (Higher energy computed structures are not reported here.) It can be seen that the interchain H-bonds (computed bond lengths N−H = 1.03 Å and H−O = 2.09 Å) have been replaced with an ionocovalent N−Zn(OH)−O cross-linkage (DFT bond lengths N−Zn = 1.94 Å and Zn−O = 2.08 Å). The computed reaction energy (including the production of ethane) is −115 kJ/mol per Zn atom relative to DEZ and H_2O in the gas phase. Upon continued processing with MPI cycles, two energetically similar reaction pathways are possible, namely, (i) continued cross-linking through the replacement of H-bonds with new ionocovalent linkages and (ii) growth of ZnO clusters at each existing Zn(OH) nucleus within the system. For one cycle of the latter process, we compute an energy gain of −113 kJ/mol per Zn (relative to gas-phase DEZ and H_2O, evolving ethane), which is close to that computed for cross-linking. We therefore predict that the final structure after repeated MPI cycles is likely to consist of a hybrid material composed of both nanoclusters of ceramic ZnO and covalently cross-linked Kevlar chains (Figure 4b).

The theoretical model is supported by the changes observed in the XRD patterns of the samples (Figure 5). Two main

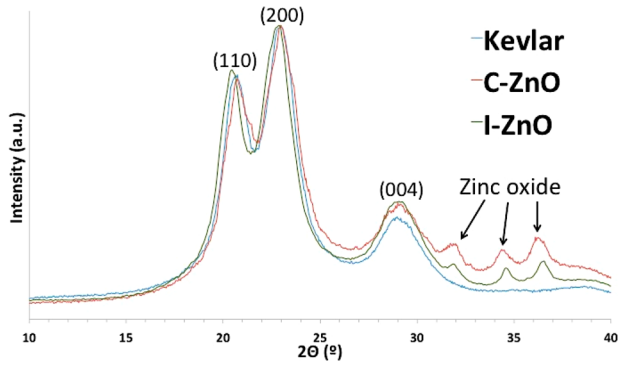

Figure 5. XRD patterns of Kevlar before and after infiltration of ZnO or coating with ZnO.

diffraction peaks can be observed in the pristine Kevlar XRD pattern, at 20.6°and 22.9°. These peaks correspond to the (110) and (200) crystal planes, respectively, which are parallel to the axis of the polymeric chain.[36,37] The positions of the peaks and their full width at half-maximum (fwhm) have been summarized in Table S1. Upon infiltration of ZnO into Kevlar a shift of both peaks toward smaller angles occurs. This shift indicates that the planes parallel to the polymeric chain stretch, thereby confirming an intercalation of ZnO. In the case of coating, a different behavior of the diffraction peaks is observed. Only a small shift toward larger angles occurs, which likely results from compressive stress induced by the inorganic coating on top of the sample. The fwhm of the coated sample increases, indicating a decrease of the crystallite size. The reduction of the crystallite size may arise from the scission of the superficial Kevlar chains resulting from the strong reactivity of the precursor and the heat evolution during the strongly exothermic reaction with water. This effect is largely compensated through cross-linking of the polymer chains with Zn in the case of the infiltrated sample.

As a result of the N−Zn−O bonding, an increase of the degradation temperature is expected. A more quantitative picture can be extracted from thermogravimetric analysis (TGA) and differential thermogravimetry (DTG) measurements as shown in Figure 6. Untreated Kevlar loses about 4% of

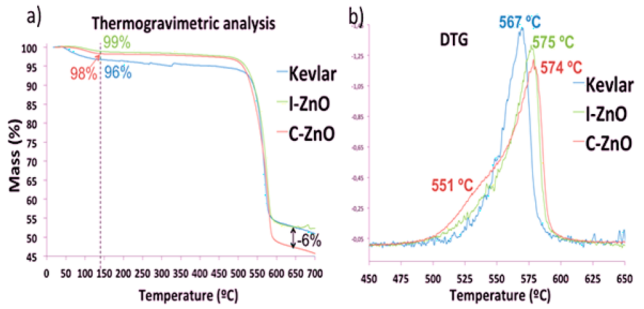

Figure 6. (a) Thermogravimetric analyses showing the mass loss of each sample as a function of temperature. (b) Derivative thermogravimetric plots showing the main degradation temperature of each sample. The temperature values of the C-ZnO sample correspond to the maxima of the deconvoluted peaks (Figure S1).

the initial mass at 150 °C (corresponding to the processing temperature), and a decomposition of the polymer occurs at 567 °C, which is in good agreement with previous studies.[38] The mass loss at 150 °C of both ZnO treated samples is similar and slightly lower than the loss observed from the untreated Kevlar. The main decomposition of these samples occurs at slightly higher temperatures (around 575 °C) than for the untreated samples. However, in the case of the C-ZnO sample a shoulder at 551 °C can be observed (deconvolution in Figure S2), which is not seen in the I-ZnO sample. This shoulder indicates that an additional decomposition process starts prior to the main decomposition, which may follow a different degradation mechanism. A very likely scenario is that upon coating with ZnO the water molecules contained within the Kevlar fibers get trapped by the coating and cannot be released at 150 °C as it occurs with untreated Kevlar. Evidence for this can be seen from the TGA curves of the samples in the early stage of heating, that is, between 50 and 150 °C. At higher temperatures the pressure of the water vapor will rise, causing the ZnO coating cracking, potentially hand in hand with a recrystallization of the ZnO. Indeed, in our earlier work we showed that temperatures of around 500 °C are sufficient to recrystallize ALD deposited ZnO on polymeric fibers.[39] The high temperatures and the presence of released water molecules will cause the C-ZnO Kevlar to start decomposing already at 520 °C.[40,41] The FTIR spectra in Figure S3 support this scenario. This additional degradation step of the C-ZnO may be responsible for the final loss in mass of 6%. The presence of smaller molecular fragments that result from chain scission, as indicated by XRD, may contribute to the enhanced mass loss and earlier induction of the degradation in the coated sample. In the I-ZnO fibers the delayed water molecule release is less expressed. The reason may be that a significant amount of water molecules within the Kevlar is consumed by the DEZ during the infiltration process; thus, the degradation process occurs in a largely inert atmosphere.

In order to seek more experimental verification of the computed structure, ATR-FTIR spectra of the samples were

DOI: 10.1021/acs.chemmater.7b03747
Chem. Mater. XXXX, XXX, XXX−XXX

measured (Figure 7). No significant differences can be observed between C-ZnO and native Kevlar. If the model of cross-linking

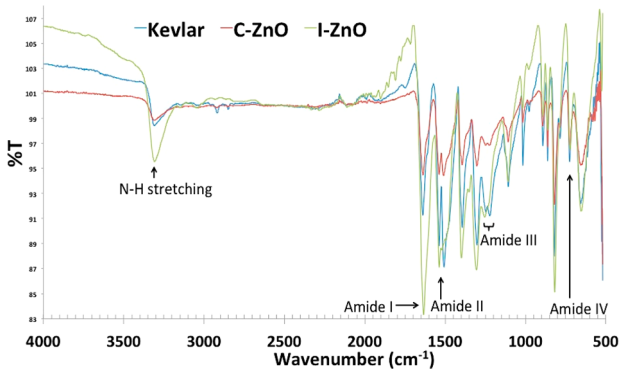

Figure 7. ATR-FTIR spectra of the various investigated samples. The peaks related to the amides are labeled.

the polymer chains with Zn holds true, the changes in the bonding structure upon infiltration with ZnO should be reflected in the FTIR spectra. It should be noted that the mole fraction of the modified area of Kevlar after infiltration is very small, and the signal of the unmodified Kevlar from the bulk of the fibers is overwhelming. Therefore, the spectra will have significant contribution from unmodified Kevlar. Nevertheless, a shift is observed from most of the amide peaks indicating that the infiltrated Zn interacts with the amide groups. The individual wavenumbers of these peaks are depicted in Table 1 for easier comparison.

Table 1. Position of the FTIR Amide Related Peaks

peak	Kevlar	C-ZnO	I-ZnO
N−H stretching	3310	3311	3306
amide I	1641	1641	1636
amide II	1539	1540	1539
amide III	1249	1250	1254
	1222	1224	1227
amide IV	727	726	721

The broadening (full width at half-maximum (fwhm) increase by 6 cm^{-1}) and red shift of the N−H stretching band after infiltration clearly show an interaction of the precursor with the amide. The theoretically predicted stretching of the C═O bond and a red shift of the corresponding peak in calculated infrared frequencies of the model are reflected in the experimentally observed redshift of the Amide I peak (a signature of stretching of C═O). The Amide II and Amide III peaks show a clear deformation compared to the peaks of the untreated Kevlar (Figure S4) in addition to the blue shift of Amide III. These peaks correspond to the coupling of two vibrational modes, N−H bending and the C−N stretching, and are commonly used to determine the secondary structure of proteins,[42−44] which can be applied to Kevlar in a similar way. The shift and shape change of the Amide II and III peaks must result from the change in the intermolecular interaction of the polymer chains and their spatial conformation, which is induced by the infiltration of ZnO into the polymer fiber. If further considering the red shift of Amide I and the blue shift of Amide III, which is dominated by the C−N stretching, this implies that a binding of Zn to the O in C═O will have a stabilizing effect on the C−N bond. In summary, the spectroscopic data is in agreement with the theoretically predicted cross-linked structure.

The enhanced stability of Kevlar against UV irradiation after infiltration is the most intriguing observation in this work. In the case of the virgin polymer, the destructive effect of UV light on the mechanical properties is a direct consequence of molecular decomposition reactions that take place on the fiber surfaces.[13,14,45] The UV light induces hydrogen bond cleavage, chain scission, and oxidation of terminal groups of the polymer. Those primarily affect the amide groups and lead to a degradation of the superficial hydrogen bonds resulting in surface etching. This effect may be enhanced if elevated temperatures are combined with UV irradiation. The superficial degradation reactions can be observed from the FTIR spectra of the Kevlar samples before and after the irradiation (Figure S5). Even though no evolution of a new peak is observed after the irradiation, the intensity of the amide related peaks changes significantly. For a clearer comparison, the spectra were normalized and the change of the intensities has been summarized in Table S2. The reduction of the intensity of the N−H stretching and Amide III bands, together with the increased intensity of the Amide I and II bands, as observed in the untreated Kevlar, arise from the cleavage of H-bonds between adjacent chains and a homolytic splitting of C−N and N−H bonds.[14,40,46] The heated Kevlar sample shows the same tendency, but the change in the intensities, especially of the N−H stretching peak, is considerably larger. In this case, the UV-induced H-bond cleavage and chain scission reactions are combined with a thermally induced H-bond cleavage. This is clearly observed from the tensile tests where the modulus of toughness of heated Kevlar after UV irradiation is even lower than in the case of untreated Kevlar. The even more pronounced loss of the mechanical properties of C-ZnO fibers after irradiation with UV light indicates that the degradation reactions are further enhanced by the ZnO coating. ZnO is known to strongly absorb UV light. The coating is therefore expected to shield the fibers from UV light and prevent radiation-induced degradation. However, for a quantitative UV blocking a film of a UV absorbing metal oxide with around 100 nm thickness is typically needed.[47,48] Since our films have only approximately half of that thickness, the UV blocking of the ZnO coating is not expected to be efficient. Furthermore, under UV illumination and in the presence of water molecules, the ZnO coating acts as a photocatalyst, creating oxygen-containing radicals that can attack the polymeric backbone. Such photocatalytic side reaction will rapidly degrade the polymer in the vicinity of the metal oxide and in this way lower the modulus of toughness. In fact, we observe the most significant loss in the modulus of toughness from coated samples after UV irradiation. The different degradation mechanism of the C-ZnO sample is also expressed in the FTIR spectra. Unlike pristine and heated Kevlar, where the changes in the N−H peak are most dominant, in this case the biggest change occurs in the Amide I peak. The increased intensity of the C═O stretching peak (Amide I) is accompanied by a shift toward higher wavenumbers as a consequence of the oxidation of the amide groups.

A similar argument may be claimed for the infiltrated samples, since ZnO is present here as well, even though it is buried in the polymer to a significant degree. However, the tensile tests show a supporting effect of the infiltrated ZnO and a suppression of the UV induced degradation. The UV protection is also reflected in the FTIR spectrum, as almost

DOI: 10.1021/acs.chemmater.7b03747
Chem. Mater. XXXX, XXX, XXX−XXX

no change in the intensities of the amide related peaks is observed. This stabilization may be explained as follows. On the one hand chain-scission reactions become less probable in the case of polymer chains that are cross-linked and stabilized with Zn. Especially with the Zn binding to amide groups, those will experience chemical stabilization and potentially shield the amide bonds from reactive molecules. On the other hand the infiltrated ZnO is buried in the subsurface area of the fiber without contact to water molecules, thus suppressing radical formation as source for UV-induced photocatalytic degradation. Most likely both effects play a partial role here and apply simultaneously.

4. CONCLUSIONS

The stability of Kevlar fibers against thermal and UV-radiation induced degradation has been significantly improved by applying a bioinspired approach, that is, by infiltration of metals into a polymeric matrix. This has been achieved through multiple pulsed infiltration of Kevlar with ZnO. As a consequence of the infiltration, a hybrid organic−inorganic material of around 30 nm thickness is created in the subsurface area of the Kevlar fibers. The structure of the hybrid material is determined by theoretical models calculated with DFT. Accordingly, the infiltrated ZnO covalently cross-links Kevlar chains and further grows inside the polymeric matrix. The shift in the vibration peaks of the amide groups observed in the FTIR spectrum indicates that the infiltrated ZnO reacts with the amide group, which is in agreement with the theoretical model. Thanks to the creation of the hybrid material the decomposition temperature of Kevlar is increased by nearly 10 °C, and 90% of its modulus of toughness is retained even after 24 h of UV irradiation, outperforming the stability of Kevlar as known by now. Thus, this new route offers the possibility to improve the stability of such high strength polymers without markedly compromising their characteristic lightness as the additional weight added by the infiltrated ZnO is negligible in comparison to the weight of the polymeric fibers. In addition, this vapor phase technique avoids the post-processing treatments that are commonly required after use of organic solvents.

■ ASSOCIATED CONTENT

Supporting Information

The Supporting Information is available free of charge on the ACS Publications website at DOI: 10.1021/acs.chemmater.7b03747.

Mechanical properties measurement setup, deconvolution of the DTG degradation peak of C-ZnO Kevlar, FTIR spectra of the decomposition gases at 520 °C, a detailed part of the ATR-FTIR spectra, FTIR spectra of the UV irradiated samples, table summarizing the peak position and fwhm of the XRD patterns of untreated, coated, and infiltrated Kevlar samples, and table summarizing the change of the intensities of the amide related peaks in the FTIR spectra of the samples after irradiation with UV light (PDF)

■ AUTHOR INFORMATION

Corresponding Author

*(M.K.) E-mail: m.knez@nanogune.eu.

ORCID

Itxasne Azpitarte: 0000-0002-4150-0816

Mato Knez: 0000-0002-9850-1035

Author Contributions

The manuscript was written through contributions of all authors. All authors have given approval to the final version of the manuscript.

Notes

The authors declare no competing financial interest.

■ ACKNOWLEDGMENTS

M.K. is grateful for funding from European Union FP7 Programme under the Grant Agreement No. 322158 (Marie Curie-CIG ARTEN) and the Spanish Ministry of Economy and Competitiveness (MINECO) within Grant Agreement No. MAT2016-77393-R, including FEDER funds. The authors acknowledge networking support within the COST action MP1402. I.A. acknowledges the Basque Government for a Ph.D. fellowship (PRE_2016_2_0022). A.L.-O. acknowledges the Spanish Ministerio de Economía y Competitividad through the Juan de la Cierva Program (IJCI-2014-21530).

■ REFERENCES

(1) Xu, X.; Heng, L.; Zhao, X.; Ma, J.; Lin, L.; Jiang, L. Multiscale Bio-Inspired Honeycomb Structure Material with High Mechanical Strength and Low Density. *J. Mater. Chem.* **2012**, *22*, 10883−10888.

(2) Reddy, N.; Yang, Y. Structure and Properties of Chicken Feather Barbs as Natural Protein Fibers. *J. Polym. Environ.* **2007**, *15*, 81−87.

(3) Rho, J.-Y.; Kuhn-Spearing, L.; Zioupos, P. Mechanical Properties and the Hierarchical Structure of Bone. *Med. Eng. Phys.* **1998**, *20*, 92−102.

(4) Martin, R. B. Determinants of the Mechanical Properties of Bones. *J. Biomech.* **1991**, *24*, 79−88.

(5) Broomell, C. C.; Mattoni, M. A.; Zok, F. W.; Waite, J. H. Critical Role of Zinc in Hardening of Nereis Jaws. *J. Exp. Biol.* **2006**, *209*, 3219−3225.

(6) Broomell, C. C.; Zok, F. W.; Waite, J. H. Role of Transition Metals in Sclerotization of Biological Tissue. *Acta Biomater.* **2008**, *4*, 2045−2051.

(7) Cribb, B. W.; Stewart, A.; Huang, H.; Truss, R.; Noller, B.; Rasch, R.; Zalucki, M. P. Unique Zinc Mass in Mandibles Separates Drywood Termites from Other Groups of Termites. *Naturwissenschaften* **2008**, *95*, 433−441.

(8) Lee, S.-M.; Pippel, E.; Gösele, U.; Dresbach, C.; Qin, Y.; Chandran, C. V.; Bräuniger, T.; Hause, G.; Knez, M. Greatly Increased Toughness of Infiltrated Spider Silk. *Science* **2009**, *324*, 488−492.

(9) Lee, S.; Pippel, E.; Moutanabbir, O.; Gunkel, I.; Thurn-albrecht, T.; Knez, M. Improved Mechanical Stability of Dried Collagen Membrane after Metal Infiltration. *ACS Appl. Mater. Interfaces* **2010**, *2*, 2436−2441.

(10) Gregorczyk, K. E.; Pickup, D. F.; Sanz, M. G.; Irakulis, I. A.; Rogero, C.; Knez, M. Tuning the Tensile Strength of Cellulose through Vapor-Phase Metalation. *Chem. Mater.* **2015**, *27*, 181−188.

(11) Abbott, N. J.; Donovan, J. G.; Schoppee, M. M. *The Effect of Temperature and Strain Rate on the Tensile Properties of Kevlar and PBI Yarns*; Defense Technical Information Center: 1974.

(12) Yue, C. Y.; Sui, G. X.; Looi, H. C. Effects of Heat Treatment on the Mechanical Properties of Kevlar-29 Fibre. *Compos. Sci. Technol.* **2000**, *60*, 421−427.

(13) Said, M. A.; Dingwall, B.; Gupta, A.; Seyam, A. M.; Mock, G.; Theyson, T. Investigation of Ultra Violet (UV) Resistance for High Strength Fibers. *Adv. Space Res.* **2006**, *37*, 2052−2058.

(14) Zhang, H.; Zhang, J.; Chen, J.; Hao, X.; Wang, S.; Feng, X.; Guo, Y. Effects of Solar UV Irradiation on the Tensile Properties and Structure of PPTA Fiber. *Polym. Degrad. Stab.* **2006**, *91*, 2761−2767.

(15) Wang, Y.; Xia, Y. M. Experimental and Theoretical Study on the Strain Rate and Temperature Dependence of Mechanical Behaviour of Kevlar Fibre. *Composites, Part A* **1999**, *30*, 1251−1257.

DOI: 10.1021/acs.chemmater.7b03747
Chem. Mater. XXXX, XXX, XXX−XXX

(16) Little, B. K.; Li, Y.; Cammarata, V.; Broughton, R.; Mills, G. Metallization of Kevlar Fibres with Gold. *ACS Appl. Mater. Interfaces* **2011**, *3*, 1965−1973.
(17) Orban, R. New Metal-Coated Fibers and Fabric Lead to Novel, Practical Products. *J. Coated Fabr.* **1989**, *18*, 246−254.
(18) Zhao, X.; Hirogaki, K.; Tabata, I.; Okubayashi, S.; Hori, T. A New Method of Producing Conductive Aramid Fibers Using Supercritical Carbon Dioxide. *Surf. Coat. Technol.* **2006**, *201*, 628−636.
(19) Conley, J.; Allman, D.; Price, D.; Mason, A. D.; Waggoner, T. J.; Smith, S. W.; Gibbons, B. Hydrothermal Synthesis of Zinc Oxide Nanowires on Kevlar Using ALD and Sputtered ZnO Seed Layers. *MRS Online Proc. Libr.* **2009**, DOI: 10.1557/PROC-1178-AA06-38.
(20) Atanasov, S. E.; Oldham, C. J.; Slusarski, K. A.; Taggart-Scarff, J.; Sherman, S. A.; Senecal, K. J.; Filocamo, S. F.; McAllister, Q. P.; Wetzel, E. D.; Parsons, G. N. Improved Cut-Resistance of Kevlar® Using Controlled Interface Reactions during Atomic Layer Deposition of Ultrathin (<50 Å) Inorganic Coatings. *J. Mater. Chem. A* **2014**, *2*, 17371−17379.
(21) Hanson, C. A.; Oldham, C. J.; Parsons, G. N. Paper Deacidification and UV Protection Using ZnO Atomic Layer Deposition. *J. Vac. Sci. Technol., A* **2012**, *30*, 01A117.
(22) Gregorczyk, K.; Knez, M. Hybrid Nanomaterials through Molecular and Atomic Layer Deposition: Top Down, Bottom Up, and in-between Approaches to New Materials. *Prog. Mater. Sci.* **2016**, *75*, 1−37.
(23) Sholl, D. S.; Steckel, J. A. *Density Functional Theory; A Practical Introduction*; John Wiley & Sons: 2002.
(24) Furche, F.; Ahlrichs, R.; Hättig, C.; Klopper, W.; Sierka, M.; Weigend, F. Turbomole. *Wiley Interdiscip. Rev. Comput. Mol. Sci.* **2014**, *4*, 91−100.
(25) Ahlrichs, R. Efficient Evaluation of Three-Center Two-Electron Integrals over Gaussian Functions. *Phys. Chem. Chem. Phys.* **2004**, *6*, 5119−5120.
(26) Weigend, F. Accurate Coulomb-Fitting Basis Sets for H to Rn. *Phys. Chem. Chem. Phys.* **2006**, *8*, 1057−1065.
(27) Treutler, O.; Ahlrichs, R. Efficient Molecular Numerical Integration Schemes. *J. Chem. Phys.* **1995**, *102*, 346−354.
(28) Eichkorn, K.; Weigend, F.; Treutler, O.; Ahlrichs, R. Auxiliary Basis Sets for Main Row Atoms and Transition Metals and Their Use to Approximate Coulomb Potentials. *Theor. Chem. Acc.* **1997**, *97*, 119−124.
(29) Peng, C. Y.; Ayala, P. Y.; Schlegel, H. B.; Frisch, M. J. Using Redundant Internal Coordinates to Optimize Equilibrium Geometries and Transition States. *J. Comput. Chem.* **1996**, *17*, 49−56.
(30) Rebouillat, S.; Escoubes, M.; Vigier, A.; Gauthier, R. Thermally Induced Changes in Kevlar Fibre Surface Evidenced by Inverse Gas Chromatography. *Polymer* **1995**, *36*, 4521−4523.
(31) Rebouillat, S.; Donnet, J.-B.; Wang, T. K. Surface Microstructure of a Kevlar Aramid Fibre Studied by Direct Atomic Force Microscopy. *Polymer* **1997**, *38*, 2245−2249.
(32) Mosquera, M. E. G.; Jamond, M.; Martinez-alonso, A.; Tascon, J. M. D. Thermal Transformations of Kevlar Aramid Fibers during Pyrolysis: Infrared and Thermal Analysis Studies. *Chem. Mater.* **1994**, *6*, 1918−1924.
(33) Vijayan, K. Effect of Enviromental Exposures on the Aramid Fibre Kevlar. *Met. Mater. Process.* **2000**, *12*, 259−268.
(34) Tanskanen, J. T.; Hägglund, C.; Bent, S. F. Correlation Growth Characteristics in Atomic Layer Deposition with Precursor Molecular Structure: The Case of Zinc Tin Oxide. *Chem. Mater.* **2014**, *26*, 2795−2802.
(35) Weckman, T.; Laasonen, K. Atomic Layer Deposition of Zinc Oxide: Diethyl Zinc Reactions and Surface Saturation from First-Principle. *J. Phys. Chem. C* **2016**, *120*, 21460−21471.
(36) Shi, Q.; Ni, L.; Zhang, Y.; Feng, X.; Chang, Q.; Meng, J. Poly(p-Phenylene Terephthamide) Embedded in a Polysulfone as the Substrate for Improving Compaction Resistance and Adhesion of a Thin Film Composite Polyamide Membrane. *J. Mater. Chem. A* **2017**, *5*, 13610−13624.
(37) Wang, P.; Wang, K.; Zhang, J.; Luo, G. Preparation of Poly(p-Phenylene Terephthalamide) in a Microstructured Chemical System. *RSC Adv.* **2015**, *5*, 64055−64064.
(38) Cai, G. M.; Yu, W. D. Study on the Thermal Degradation of High Performance Fibers by TG/FTIR and Py-GC/MS. *J. Therm. Anal. Calorim.* **2011**, *104*, 757−763.
(39) Kim, G.; Lee, S.; Knez, M.; Simon, P. Single Phase ZnO Submicrotubes as a Replica of Electrospun Polymer Fi Ber Template by Atomic Layer Deposition. *Thin Solid Films* **2014**, *562*, 291−298.
(40) Liu, X.; Yu, W. Evaluating the Thermal Stability of High Performance Fibers by TGA. *J. Appl. Polym. Sci.* **2006**, *99*, 937−944.
(41) DuPont. *KEVLAR Aramid Fiber: Technical Guide*; 2011.
(42) Cai, S.; Singh, B. R. Identification of Beta -Turn and Random Coil Amide III Infrared Bands for Secondary Structure Estimation of Proteins. *Biophys. Chem.* **1999**, *80*, 7−20.
(43) Cai, S.; Singh, B. R. A Distinct Utility of the Amide III Infrared Band for Secondary Structure Estimation of Aqueous Protein Solutions Using Partial Least Squares Methods. *Biochemistry* **2004**, *43*, 2541−2549.
(44) Singh, B. R.; Deoliveira, D. B.; Fu, F.; Fuller, M. P. Fourier Transform Infrared Analysis of Amide III Bands of Proteins for the Secondary Structure Stimation. *Proc. SPIE* **1993**, *1890*, 47−55.
(45) Wang, H.; Xie, H.; Hu, Z.; Wu, D.; Chen, P. The Influence of UV Radiation and Moisture on the Mechanical Properties and Micro-Structure of Single Kevlar Fibre Using Optical Methods. *Polym. Degrad. Stab.* **2012**, *97*, 1755−1761.
(46) Liu, X.; Yu, W.; Pan, N. Evaluation of High Performance Fabric Under Light Irradiation. *J. Appl. Polym. Sci.* **2011**, *120*, 552−556.
(47) Xiao, X.; Liu, X.; Fang, D.; Zhang, C.; Xia, L.; Xu, W.; Chen, F. Highly Anti-UV Properties of Silk Fiber with Uniform and Conformal Nanoscale TiO_2 Coatings via Atomic Layer Deposition. *ACS Appl. Mater. Interfaces* **2015**, *7*, 21326−21333.
(48) Chen, W.; Qian, X.; He, X.; Liu, J. Enhanced Ultraviolet Resistance of Kevlar Fibers with TiO_2 Films. *Reliab. Maintainab. Saf. 9th Int. Conf.* **2011**, 1267−1272.

DOI: 10.1021/acs.chemmater.7b03747
Chem. Mater. XXXX, XXX, XXX−XXX